

Electron-electron scattering effects on the Full Counting Statistics of Mesoscopic Conductors

S. Pilgram

Département de Physique Théorique, Université de Genève, CH-1211 Genève 4, Switzerland

(Dated: October 29, 2018)

In the hot electron regime, electron-electron scattering strongly modifies not only the shot noise but also the full counting statistics. We employ a method based on a stochastic path integral to calculate the counting statistics of two systems in which noise in the hot electron regime has been experimentally measured. We give an analytical expression for the counting statistics of a chaotic cavity and find that heating due to electron-electron scattering renders the distribution of transmitted charge symmetric in the shot noise limit. We also discuss the frequency dispersion of the third order correlation function and present numerical calculations for the statistics of diffusive wires in the hot electron regime.

PACS numbers: 73.23.-b, 05.40.-a, 72.70.+m, 24.60.-k

I. INTRODUCTION

During the last ten years, nonequilibrium noise measurements have become a standard tool in mesoscopic physics, because they reveal additional information about mesoscopic conductors beyond linear response¹. Recently, even further experimental progress has been made: Reulet, Senzier and Prober measured for the first time successfully the third moment of current statistics of a tunnel junction². They discovered a surprising temperature dependence of the third moment which was explained by the backaction of the resistive measurement device on the junction³.

Nonequilibrium noise and third moment of current fluctuations are part of a more general concept, the full counting statistics (FCS) which is defined as the probability distribution of charge that passed an electric conductor during a measurement. The introduction of FCS into mesoscopic physics by Levitov and Lesovik⁴ one decade ago has inspired a lot of theoretical work. Whereas early work concentrated mainly on noninteracting systems, recent publications developed schemes which include effects due to Coulomb interactions. Most of these works consider correlated electron systems in which intrinsic^{5,6,7} or environmental^{8,9} Coulomb blockade plays a central role. However, Coulomb interactions are important as well for the FCS of semiclassical systems: At low temperatures in the hot electron regime, electron-electron scattering leads to a local thermalization of the electron gas. Since inelastic electron-phonon scattering is strongly suppressed, the local electron temperature may be different from the lattice temperature and is allowed to fluctuate. These temperature fluctuations modify the intensity of current noise and therefore influence the FCS.

Nonequilibrium noise in the hot electron regime has first been measured in diffusive wires¹⁰. Since heating effects are difficult to avoid, it only became possible later to extend these measurements to the cold electron regime in which electron-electron scattering is absent¹¹. Similar noise experiments in the hot electron regime have been carried out in great detail on chaotic cavities¹² and chains

of cavities¹³.

The measured Fano factors in all cited experiments can be entirely explained by theories based on the semiclassical Boltzmann-Langevin formalism^{14,15,16,17}, since both Coulomb blockade and quantum interference were unimportant. Although the third cumulant of FCS of a diffusive wire in the hot electron regime was obtained quantum mechanically¹⁸, it is clearly desirable to have a fully semiclassical method to treat the FCS of semiclassical systems. An important step in this direction has been undertaken in Ref. 19 where a diagrammatic scheme for higher order cumulants has been proposed. A theory for the full charge distribution of FCS based on a stochastic path integral was then presented in Ref. 20 and extended to time-dependent correlation functions in Ref. 21. It is the aim of this article to apply the stochastic path integral approach to systems in the hot electron regime.

This article is organized as follows: The first geometry under consideration, the chaotic cavity, is introduced in Sec. II. The principal tools to obtain the FCS for this system are discussed in Secs. II B and II C, results are presented in Secs. II D and II E. In Sec. III, we compare the statistics of cavity and diffusive wire and give in the conclusions IV some estimates which show that our calculations are relevant for experiments.

II. CHAOTIC CAVITY

A. the model

The system we study in this section is shown in the upper panel of Fig. 1. A chaotic cavity is a conducting island of irregular shape. Its properties are essentially defined by two quantities, the mean spacing of electron levels $\Delta = N_F^{-1}$ and the capacitance C_g which describes the Coulomb interaction of the cavity and its environment represented by a nearby gate. The island is connected to external leads by two point contacts. These openings are chosen to be small compared to the size of the cavity in order to keep motion inside the cavity

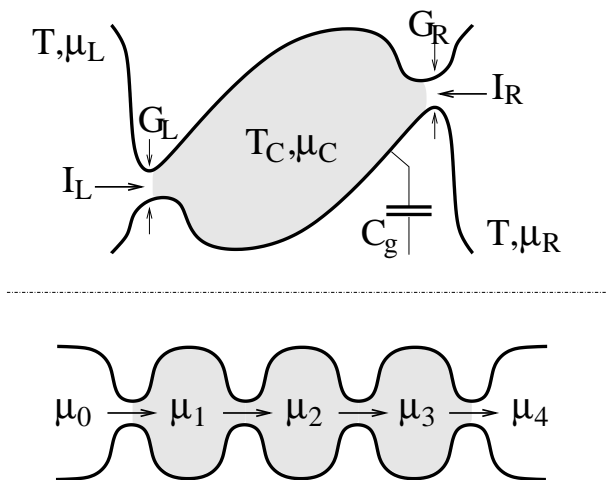


FIG. 1: The two geometries under consideration in this article. *Upper panel:* A chaotic cavity in the hot electron regime which is characterized by a fluctuating effective chemical potential μ_C and an effective temperature T_C . *Lower panel:* A chain of N cavities which mimics in the large N limit a diffusive wire.

chaotic. The leads are assumed to be in local thermal equilibrium described by Fermi distribution functions $f_{L,R}(\varepsilon) = \{1 + \exp[(\varepsilon - \mu_{L,R})/T]\}^{-1}$ (here and in the following, we set $\hbar = 1$, $e = 1$ and $k_B = 1$).

Depending on the conductances $G_{L,R}$ of the two point contacts, this system shows despite of its conceptual simplicity a rich variety of physical regimes: For low dimensionless conductance $G_{L,R} \ll 1$, the charge transport through the cavity is dominated by Coulomb blockade effects and may exhibit Kondo physics²². For intermediate conductance $1 \lesssim G_{L,R}$, weak Coulomb blockade is still possible if temperature and applied voltage $\mu = \mu_L - \mu_R$ are small enough. Furthermore, the conductance of the cavity is subject to weak localization corrections²³. In the semiclassical regime $G_{L,R} \gg 1$, signatures of the quantum nature of the charge carriers disappear completely in measurements of mean currents. The total conductance of the cavity is now simply given by Ohm's law, i.e. by the conductance of the two point contacts in series ($G = G_L G_R / (G_L + G_R)$). However, even in this semiclassical limit, the quantum statistics of the electrons has a strong influence on transport fluctuations, namely on the shot noise produced by the two point contacts. For simplicity, we will assume that both contacts are completely open, i.e. no backreflection is taking place at the point contacts.

In the semiclassical regime, the state of the cavity is characterized by its time-dependent electron occupation function $f_C(\varepsilon - U_C)$ and the electrostatic potential U_C . The chaotic scattering inside the cavity renders this occupation function position independent and isotropic²⁴. Due to the random nature of the currents flowing into the cavity, the occupation function $f_C(\varepsilon - U_C)$ is fluctu-

ating around its mean $f_C^0(\varepsilon)$. There are four time scales which are important for the dynamics of these fluctuations: The electron-electron scattering time τ_{e-e} , the inelastic scattering time τ_{e-ph} , the dwell time $\tau_d = R_q N_F$ which is the time an electron spends inside the cavity, and the rc-time $\tau_{rc} = R_q C_\mu$ that describes the relaxation of charged fluctuations inside the cavity. Here, $R_q = (G_L + G_R)^{-1}$ denotes the charge relaxation resistance and $C_\mu^{-1} = C_g^{-1} + N_F^{-1}$ is the electrochemical capacitance of the cavity²⁵. The mean occupation function $f_C^0(\varepsilon)$ depends on the relations between the different time scales: In the *cold electron regime* ($\tau_{e-ph} \gg \tau_{e-e} \gg \tau_d$), the energy of every electron passing the cavity is conserved. Particle current conservation at each energy implies $f_C^0 = R_q (G_L f_L + G_R f_R)$. Shot noise in this regime has been first characterized by random matrix theory²⁶ using the scattering theory of noise^{27,28,29} and later by a semiclassical approach^{30,31}. Higher cumulants have been calculated quantum mechanically for open point contacts³² and semiclassically for arbitrary contacts³³. In the *dissipative regime* ($\tau_d \gg \tau_{e-ph}$), electrons entering the cavity are in thermal equilibrium with the surrounding phonon bath and only the energy integrated particle current through the cavity is conserved. Noise for this regime has been calculated from a voltage probe model³⁰ and recently for low bias in the framework of circuit theory⁷. In the *hot electron regime* ($\tau_{e-ph} \gg \tau_d \gg \tau_{e-e}$), both particle current and total energy current through the cavity are conserved (for theoretical predictions of noise see Ref. 12,16). The distribution of the electrons in the cavity is described by a Fermi function $f_C(\varepsilon) = \{1 + \exp[(\varepsilon - \mu_C)/T_C]\}^{-1}$ where both electrochemical potential μ_C and local electron temperature T_C are fluctuating around their mean values μ_C^0 and T_C^0 . Notice that there is no experimental distinction between these three regimes on the level of mean current. Only noise measurements reveal the type of interactions present in the cavity. From now on, we will focus on the hot electron regime.

B. preliminaries

Before we start to describe the calculation of the FCS, we give a brief summary of definitions we use throughout the paper. The complete information about the statistics of current flow $I(t)$ through a cross section of a conductor is contained in its probability functional $P_I[I(t)]$. More general, the probability functional to find a certain realization of a stochastic variable $A(t)$ defined on the interval $[0, \tau]$ can be written as Fourier transform

$$P_A[A] = \int \mathcal{D}\chi_A \exp \left\{ -i \int_0^\tau \chi_A A + S_A[i\chi_A] \right\} \quad (1)$$

where we introduced the characteristic functional $S_A[\chi_A(t)]$, the conjugated field $\chi_A(t)$, and a functional integration over the measure $\mathcal{D}\chi_A$. An analytic continuation of $S_A[\chi_A(t)]$ to an imaginary field $i\chi_A$ is used for

the Fourier transformation in Eq. (1). Functional derivatives of the characteristic functional yield the irreducible part of any correlation function

$$\langle A(t_1) \dots A(t_n) \rangle = \frac{\delta^n S_A[\chi_A(t)]}{\delta \chi_A(t_1) \dots \delta \chi_A(t_n)} \Big|_{\chi_A=0} \quad (2)$$

in time representation. Often, one is interested in the behavior of stationary systems. It is then useful to introduce the spectral function $C_A^n(\omega_1, \dots, \omega_{n-1})$ which is linked to the Fourier transform of the correlation function (2) by

$$\langle A(\omega_1) \dots A(\omega_n) \rangle = 2\pi \delta(\omega_1 + \dots + \omega_n) C_A^n(\omega_1, \dots, \omega_{n-1}). \quad (3)$$

The full counting statistics of charge transfer as defined by Levitov et al.⁴ does not keep the entire information contained in the functional $S_I[\chi_I]$ for current fluctuations, but retains only the probability distribution of the time integrated current

$$P(Q) = \int d\chi e^{-i\chi Q + S(i\chi)}, \quad Q = \int_0^\tau dt I(t). \quad (4)$$

The characteristic function $S(\chi)$ of FCS is obtained from the complete functional $S_I[\chi_I]$ by choosing $\chi_I(t) = \chi$. The counting field χ is constant in time. The distribution $P(Q)$ may be connected to the spectral function of the current C_I^n . In the long-time limit for instance, the cumulants of the FCS $P(Q)$ turn out to be the spectral functions τC_I^n taken at zero frequency.

C. calculations

In this section, we discuss the essential steps that are necessary to calculate the transport statistics in the presence of strong electron-electron scattering. We employ a stochastic path integral formalism which has been developed in Ref. 20 to study the FCS of semiclassical mesoscopic conductors. This formalism is based on the observation that the correlation time of bare current fluctuations in the point contacts is the shortest time scale in the problem. This allows us to proceed in two steps: First, we consider the point contacts as sources of white noise which obey statistics that depend on external parameters such as the occupation functions of the leads and the cavity. Second, we identify a set of conserved currents which allow us to determine the adiabatic time evolution of the external parameters. To characterize the bare noise of the point contacts we introduce characteristic functionals $S_j[\chi_j, \xi_j]$ for the current fluctuations in each contact (see Eq. (1))

$$S_j[\chi_j, \xi_j] = \int_0^\tau H_j(\chi_j, \xi_j, \mu_j, T_j, \mu_C, T_C) d\tau \quad j = L, R. \quad (5)$$

The fields χ_j and ξ_j are conjugated to particle current $I_j^p(t)$ and total energy current $I_j^e(t)$ respectively. The

Fourier transform of $\exp\{S_j\}$ is the probability functional $P_j[I_j^p, I_j^e]$ to find a certain realization of currents. The white color of the noise is apparent from the form of Eq. (5) which contains one single time integration; probabilities at different times are hence independent. The precise form of H_j must be taken from a quantum mechanical calculation. With the help of Ref. 4, one finds for open point contacts^{20,34}

$$H_j(\chi_j, \xi_j) = G_j \int d\varepsilon \ln [1 + f_j(\varepsilon) (e^{\chi_j + \varepsilon \xi_j} - 1)] + G_j \int d\varepsilon \ln [1 + f_C(\varepsilon) (e^{-\chi_j - \varepsilon \xi_j} - 1)]. \quad (6)$$

Since all occupation functions in Eq. (6) are Fermi functions, the energy integrals over ε remain elementary. The generating functions of the point contacts as a function of temperature T_C and chemical potential μ_C of the cavity are given by

$$H_j(\lambda, \xi, V_j, V_C, T_j, T_C) = \frac{\pi^2 G_j}{6} \frac{2V_j \lambda + T_j \lambda^2 + ((T_j)^2 + (V_j)^2) \xi}{1 - T_j \xi} - \frac{\pi^2 G_j}{6} \frac{2V_C \lambda - T_C \lambda^2 + ((T_C)^2 + (V_C)^2) \xi}{1 + T_C \xi}. \quad (7)$$

To shorten the expressions, we have rescaled the chemical potentials $\mu_j = \pi V_j / \sqrt{3}$ and the fields $\chi_j = \pi \lambda_j / \sqrt{3}$.

Now that we have solved the problem of charge and energy transfer statistics through each individual point contact, we can proceed to determine the more difficult statistics for two point contacts in series. To this end, we need to find conservation laws that set the slow dynamics of the two variables μ_C and T_C which define the state of the cavity in the hot electron regime. We therefore combine the conservation of charge Q_C and total energy E_C inside the cavity

$$\dot{Q}_C = I_L^p + I_R^p \quad \dot{E}_C = I_L^e + I_R^e \quad (8)$$

with expressions that link the conserved quantities to chemical potential and temperature

$$Q_C = C_\mu \mu_C \quad E_C = \frac{\pi^2}{6} N_F (T_C)^2 + \frac{1}{2} C_\mu (\mu_C)^2. \quad (9)$$

These relations include charge screening inside the cavity on the level of the Thomas-Fermi approximation²⁵. The conservation laws (8) are conveniently expressed by Lagrange multipliers χ_C and ξ_C which are introduced through delta-functionals in Fourier representation. We use

$$\delta [I_L^p + I_R^p - \dot{Q}_C] = \quad (10)$$

$$\int \mathcal{D}\chi_C \exp \left\{ -i \int_0^\tau dt \chi_C (I_L^p + I_R^p - \dot{Q}_C) \right\}$$

for the charge conservation and a similar expression for the energy conservation. Without incorporating the conservation laws (8), the probability to find a certain realization of particle and energy currents is given by the

product $P_L[I_L^p, I_L^e]P_R[I_R^p, I_R^e]$, i.e. the left and the right point contact are independent. We combine this product with the delta-functional (10) and construct a conditional probability

$$P[I_L^p, I_R^p, I_L^e, I_R^e] = \int \mathcal{D}Q_C \mathcal{D}E_C \delta \left[I_L^p + I_R^p - \dot{Q}_C \right] \delta \left[I_L^e + I_R^e - \dot{E}_C \right] P_L[I_L^p, I_L^e] P_R[I_R^p, I_R^e] \quad (11)$$

which satisfies the current conservation laws. Introducing the characteristic functionals (5) of the point contacts, we find that the total characteristic functional for the cavity can be written as stochastic path integral²⁰

$$e^{\tilde{S}_I[i\chi_I]} = \int \mathcal{D}Q_C \mathcal{D}E_C \mathcal{D}\chi_C \mathcal{D}\xi_C e^{S_I[i\chi_I, i\chi_C, i\xi_C, Q_C, E_C]} \quad (12)$$

over the action

$$S_I[\chi_I, \chi_C, \xi_C, Q_C, E_C] = \int_0^\tau dt \left(-(\chi_C \dot{Q}_C + \xi_C \dot{E}_C) + H_L(\chi_C + \chi_I, \xi_C) + H_R(\chi_C, \xi_C) \right). \quad (13)$$

In the semiclassical regime, this path integral may be evaluated in saddle point approximation ($\tilde{S}_I = S_I$ at the saddle point). Due to the adiabatic evolution of the chemical potential μ_C and the effective temperature T_C of the cavity, Gaussian corrections are small²⁰. The four saddle point equations get the form

$$\begin{aligned} \dot{Q}_C &= \frac{\partial H_L}{\partial \chi_C} + \frac{\partial H_R}{\partial \chi_C}, & \dot{E}_C &= \frac{\partial H_L}{\partial \xi_C} + \frac{\partial H_R}{\partial \xi_C}, \\ \dot{\chi}_C &= -\frac{\partial H_L}{\partial Q_C} - \frac{\partial H_R}{\partial Q_C}, & \dot{\xi}_C &= -\frac{\partial H_L}{\partial E_C} - \frac{\partial H_R}{\partial E_C}, \end{aligned} \quad (14)$$

and resemble formally the canonical equations of motion for position and momentum in mechanics. The first two equations can be interpreted as continuity equations that express the change of charge and energy in the cavity in terms of incoming currents. The right sides of third and fourth equation can be understood as forces which prevent the saddle point solutions from exploring unlikely regions of the configuration space.

D. results

In this section, we evaluate Eq. (13) in the zero frequency limit. In this case, we may set all time derivatives in the action (13) and the saddle point equations (14) to zero. The external counting field $\chi_I(t) = \chi$ becomes time independent and is conjugated to the charge transmitted through the cavity during time τ ; i.e. $S(\chi) = S_I[\chi]$ generates the FCS (see Eq. (4)). We are left with a system of four nonlinear equations (14) to be solved. It turns out that analytical solutions to this system exist. After inserting these solutions into Eq. (13) we arrive at the

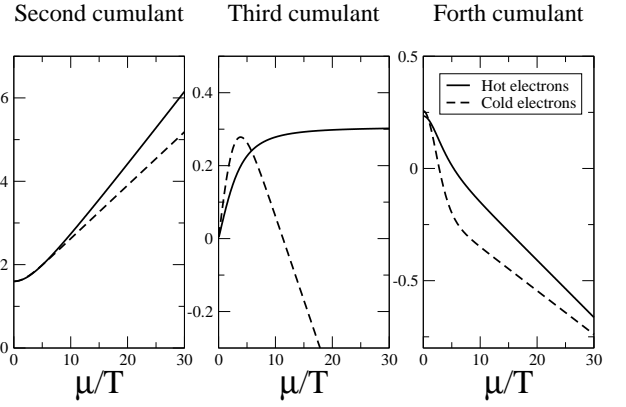


FIG. 2: Comparison of hot and cold electron regime: The cumulants of counting statistics are plotted as a function of the applied bias μ for an asymmetric cavity ($\eta = 2/5$). The biggest difference appears in the third cumulant which does not change sign in the presence of electron-electron scattering.

following result for the generating function of FCS which is valid in the long-time limit ($G\tau \max\{\mu, T\} \gg 1$)

$$S(\tilde{\chi}) = \frac{\pi^2}{3} G\tau \left[V\tilde{\chi} + \left(\sqrt{\eta^{-2} + \tilde{\chi}^2} - \eta^{-2} \right) \times \left(T\sqrt{\eta^{-2} + \tilde{\chi}^2} + \sqrt{T^2(\eta^{-2} + \tilde{\chi}^2) + V^2 + 2TV\tilde{\chi}} \right) \right]. \quad (15)$$

The ratio $\eta = \sqrt{G_L G_R} / (G_L + G_R)$ describes the asymmetry of the cavity and becomes at most 1/2 in the case of a symmetric cavity; $G = G_L G_R / (G_L + G_R)$ is the conductance of the cavity. We remind the reader that we have rescaled the bias $V = \pi\mu/\sqrt{3}$ and the counting field $\tilde{\chi} = \pi\chi/\sqrt{3}$. Cumulants of transmitted charge $Q = \int_0^\tau dt I(t)$ can be obtained from derivatives of Eq. (15) with respect to χ . For the first few cumulants τC_I^n one finds

$$C_I^1 = G\mu, \quad C_I^2 = G(T + T_C^0),$$

$$C_I^3 = \frac{9}{\pi^2} \frac{G^2}{G_L + G_R} \frac{T\mu}{T_C^0},$$

$$C_I^4 = \frac{9}{\pi^2} \frac{G^2}{G_L + G_R} \left(T - T_C^0 + \frac{2T^4}{(T_C^0)^3} \right). \quad (16)$$

The mean effective temperature of the cavity is $(T_C^0)^2 = T^2 + \pi^2 \eta^2 \mu^2 / 3$. The average current C_I^1 is obtained from Ohm's law, the noise C_I^2 has been first calculated in Refs. 12,16 and third and fourth cumulant were obtained in a perturbative manner in Ref. 20. The cumulants are shown as a function of applied voltage in Fig. 2 and are compared to the same cumulants in the cold electron regime³⁵. The asymmetry is chosen to be $\eta = 2/5$. Several conclusions can be drawn from Fig. 2 and Eqs. (15,16):

- Whereas even cumulants behave qualitatively similar in both regimes, odd cumulants are strongly suppressed in the shot noise limit of the hot electron regime. This can be immediately seen in Eq. (15). There are only two terms which are odd in the counting field $\tilde{\chi}$. The first term is responsible for the mean current only, and the second term in the square root is irrelevant for high voltages (shot noise) and for low voltages (thermal noise). An asymmetry in the distribution of transmitted charge thus only appears in an intermediate regime. Qualitatively, this symmetrization can be explained by the argument that the hot electron regime is closer to thermal equilibrium where odd cumulants vanish.
- In both regimes, the third cumulant carries the same sign as the first cumulant for low voltage. However, for high voltages the third cumulant in the cold electron regime changes sign. (Such a sign change does not exist for two tunnel junctions in series). For cold electrons, the sign change can be understood from the distribution of transmission eigenvalues. In the hot electron regime, a careful analysis of cascade corrections^{19,33} shows that positive correlations between electron temperature T_C and charge currents are at the origin of this sign.
- The transition from low to high bias is smoother in the hot electron regime: The formulas contain square root laws in contrast to the cold electron regime where the transition is described by exponential laws.
- Even and odd cumulants close to equilibrium are linked by a generalized fluctuation-dissipation theorem³⁶

$$2T \frac{\partial C_I^{n-1}}{\partial \mu} = C_I^n \text{ at } \mu = 0. \quad (17)$$

In the long-time limit, the probability distribution of transmitted charge which is the Fourier transform of Eq. (15) can be calculated in saddle point approximation. The upper left panel of Fig. 4 shows the probability distribution for low bias, high bias and for an intermediate regime where the distribution becomes asymmetric. An analytical result is available in the shot noise limit. We find

$$P(Q) \sim \exp \left\{ \frac{\pi \bar{Q}}{\sqrt{3}\eta} \left(1 - \sqrt{\frac{Q}{\bar{Q}} \left(2 - \frac{Q}{\bar{Q}} \right)} \right) \right\}, \quad (18)$$

i.e. the logarithm of the distribution in the long time limit corresponds to a semicircle drawn around the mean charge $\bar{Q} = G\tau\mu$.

E. frequency dispersion

In this section, we go beyond the FCS and calculate the frequency dependence of the third order correlation function (2). To this end, we solve the saddle point equations (14) for a time dependent external field $\chi_I(t)$. The solution has to be found in a perturbative manner: First, the response of all internal fields $\chi_C, \xi_C, \mu_C, T_C$ to the external field χ_I is calculated up to quadratic order using the four saddle point equations (14). Second, the internal fields are inserted into the action (13). All terms in the action which are of third order in the external field will contribute to the desired correlation function (for details of the calculation see Ref. 21 where the same calculation for the cold electron regime is discussed thoroughly).

There is a substantial difference between the noise correlator and higher order correlation functions which was first pointed out in Ref. 21. Dispersion in the noise correlator appears only at high frequencies given by the inverse rc-time $(\tau_{rc})^{-1}$ and is therefore difficult to measure. Higher order correlators however, exhibit dispersion already on a scale given by the inverse dwell time $(\tau_d)^{-1}$ which is a much lower frequency in metallic systems. Physically, this dispersion is due to slow fluctuations of the electron temperature T_C which do not show up in the noise correlator, but couple back into higher cumulants. Such charge-neutral temperature fluctuations cannot be relieved by particle currents. The only relaxation mechanism for these fluctuations is heat flow which reacts on the time scale τ_d .

For the noise correlator in the hot electron regime we find

$$C_I^2(\omega) = G (T + T_C^0) \Delta_2. \quad (19)$$

This is the auto correlation function of currents in the left lead. The dispersion is described by the expression

$$\Delta_2(\omega) = \left(1 + \frac{2\omega^2\tau_{rc}^2}{1 - \sqrt{1 - 4\eta^2}} \right) / \left(1 + \omega^2\tau_{rc}^2 \right) \quad (20)$$

which depends only on the rc-time τ_{rc} and the asymmetry parameter η . At low frequencies, C_I^2 describes correlated noise of left and right point contact and reduces to Eq. (16) for $\omega = 0$. At high frequencies, the statistics of the two point contacts become independent, C_I^2 is then equal to the bare noise of the left contact.

The general result for the third order correlation function is too long to be presented here. We only give the experimentally relevant behavior at low frequencies ($\omega_{1,2} \ll (\tau_{rc})^{-1}$)

$$C_{I,\text{hot}}^3(\omega_1, \omega_2) = \frac{9}{\pi^2} \frac{G^2}{G_L + G_R} \frac{T\mu}{T_C^0} \Delta_3. \quad (21)$$

The dispersion at low frequencies is independent of the asymmetry parameter η and given by

$$\Delta_3(\omega_1, \omega_2) = \frac{1 + (\omega_1^2 + \omega_2^2 + \omega_1\omega_2) \tau_d^2/3}{(1 - i\omega_1\tau_d)(1 - i\omega_2\tau_d)(1 + i(\omega_1 + \omega_2)\tau_d)}. \quad (22)$$

It is important to note that charge pile up inside the cavity is forbidden on time scales longer than the re-time. Therefore, these current fluctuations are the same in both point contacts.

For comparison, we also give the third order correlation function of the cold electron regime (the zero temperature result has been calculated in Ref. 21 for more general cavities with backscattering at the point contacts)

$$C_{I,\text{cold}}^3(\omega_1, \omega_2) = M + \frac{3G^2}{G_L + G_R} \frac{T \sinh(\mu/T) - \mu}{\cosh(\mu/T) - 1} \Delta_3 \quad (23)$$

where M is a contribution which is independent of frequency

$$M = \frac{G (G_L^2 + G_R^2) (G_L - G_R)^2}{(G_L + G_R)^4} \times \frac{2\mu + \mu \cosh(\mu/T) - 3T \sinh(\mu/T)}{\cosh(\mu/T) - 1}. \quad (24)$$

Note that the low-frequency dispersion $\Delta_3(\omega_1, \omega_2)$ of the third order correlation function (22) is the same as in the cold electron regime. Also the prefactors of $\Delta_3(\omega_1, \omega_2)$ are similar: They both vanish at zero temperature and at zero bias, i.e. they are proportional to the minimum of temperature and bias.

III. DIFFUSIVE WIRE

So far we considered heating effects on current statistics in semiclassical chaotic cavities. It was particularly easy to introduce the stochastic path integral formalism to the reader on a geometry which is essentially zero-dimensional. Moreover, heating effects on noise in this geometry have been measured¹². Nevertheless, it is an important question whether part of our observations do also apply to other systems in which electron-electron scattering is strong. In fact, noise in the hot electron regime was first theoretically studied^{14,15} and experimentally verified^{10,11} in diffusive wires. It therefore seems natural to extend our theory to diffusive systems and to compare the results to the chaotic cavity.

To derive an action similar to Eq. (13) for a diffusive wire, we consider first a chain of cavities connected by identical point contacts (see lower panel of Fig. 1). Every cavity is capacitively coupled to a close gate. Such a chain has been studied experimentally and theoretically in Ref. 13. In a second step, we take the continuous limit of a large number N of cavities, but keep the total conductance constant. The continuous limit corresponds to a diffusive wire with short range Coulomb interaction (short screening length), since we have neglected capacitances between neighboring cavities. The action for the chain is given by

$$S = \tau \sum_{n=0}^{N-1} H(\lambda_{n+1} - \lambda_n, \xi_{n+1} - \xi_n, V_n, V_{n+1}, T_n, T_{n+1}) \quad (25)$$

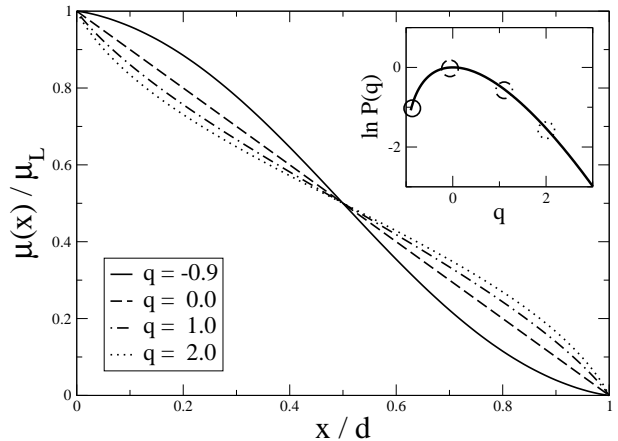


FIG. 3: Saddle point solutions to the action (26) of a diffusive wire in the hot electron regime: The inset shows the probability distribution $P(q)$ of transmitted charge through a wire in the hot electron regime in the shot noise limit. The charge is normalized as $q = Q/(G\mu\tau)$ and the mean charge has been subtracted. For four selected values of q , we plot the corresponding saddle point solution for the mean chemical potential $\mu(x)$ inside a wire of length d .

where H of each point contact is defined by Eq. (7). Each cavity ($n = 1..N - 1$) is characterized by its rescaled chemical potential $V_n = \sqrt{3}\mu_n/\pi$ and its effective temperature T_n . Energy and charge in each cavity obey conservation laws that are guaranteed by the fields λ_n and ξ_n . The labels $n = 0, N$ belong to the reservoirs. To calculate the characteristic function $S(\chi)$ of FCS, we choose the boundary conditions $\xi_0 = \xi_N = \lambda_0 = 0$ and $\lambda_N = \sqrt{3}\chi/\pi$ for the counting fields, $\mu_0 = \mu$, $\mu_N = 0$ for the chemical potentials and $T_0 = T_N = T$ for the temperature. The action (25) has then to be varied with respect to all internal fields to obtain $4N - 4$ coupled nonlinear saddle point equations.

In the continuous limit $N \rightarrow \infty$, the difference between neighboring fields n and $n + 1$ becomes infinitesimal and the sum in Eq. (25) may be replaced by an integral. We obtain the action of a nonlinear field theory

$$S = \tau \int_0^d dx \left\{ (\lambda' \ \xi') \hat{A} \begin{pmatrix} \lambda' \\ \xi' \end{pmatrix} + (\lambda' \ \xi') \hat{B} \begin{pmatrix} V' \\ T' \end{pmatrix} \right\}. \quad (26)$$

The first matrix

$$\hat{A} = \frac{\pi^2 \sigma}{3} \begin{pmatrix} T & VT \\ VT & V^2 T + T^3 \end{pmatrix} \quad (27)$$

expresses the noise intensity in local equilibrium. The second matrix

$$\hat{B} = \frac{\pi^2 \sigma}{3} \begin{pmatrix} 1 & 0 \\ V & T \end{pmatrix}. \quad (28)$$

is the linear response tensor, σ denotes the one-dimensional conductance.³⁷

At this point, it seems appropriate to discuss the approximations made in the derivation of Eq. (26). Since the action for the diffusive wire was constructed from the continuous limit of a very specific model, a chain of cavities linked by open point contacts, one might question the validity of our “back of the envelope” derivation that we employed for simplicity. It turns out that Eq. (26) may be obtained as well from a detailed microscopic calculation based on the Boltzmann-Langevin approach^{14,15}, if we apply the standard diffusion approximation and assume the conductor to be quasi-one-dimensional. Even without referring to the Boltzmann equation, it can be checked that the continuous limit of the action (25) does not depend on the details of the chain (which may as well contain point contacts of arbitrary energy independent transparency). In general, the conductance σ then becomes coordinate dependent. We made however an approximation in neglecting the possible energy dependence of the transparency of the point contacts. Including such a dependence adds an off-diagonal element $\hat{B}_{12} \neq 0$ to the linear response tensor, i.e. temperature gradients then generate a particle flow. Such an additional term implies that the Wiedemann-Franz law is no longer valid and that the Fano factor of shot noise becomes non-universal¹⁷. Since there is no trace of such a non-universality in the experiments on noise in diffusive wires^{10,11} and in the chain of cavities¹³, we disregard this additional term.

Note that the action (26) is quadratic in the fields λ, ξ , i.e. in the gradient expansion we lost all informations about higher order correlators of the elementary noise sources (the point contacts). This property is not restricted to the hot electron regime, but is a consequence of the diffusion approximation and the assumption that there are no long range interactions leading to displacement currents. Furthermore, all terms in the action (26) depend only on x-derivatives λ', ξ' . Therefore, the saddle point equations which are obtained from varying Eq. (26) with respect to λ and ξ take the form of continuity equations for charge and energy conservation. Their solutions are easily found for the special boundary condition $\chi = 0$. We obtain the profiles of mean chemical potential and mean effective temperature in the wire

$$\begin{aligned} V^0 &= V_L \left(1 - \frac{x}{d}\right) \\ (T^0)^2 &= T^2 + V_L^2 \left(1 - \frac{x}{d}\right) \frac{x}{d}. \end{aligned} \quad (29)$$

The comparison of this result with Refs. 14,15 serves as a check for our calculation. For general counting field $\chi \neq 0$, the saddle point equations form a set of coupled nonlinear diffusion equations. We have used the discretized version of the action (25) to solve these equations and to obtain the FCS numerically³⁸.

Exemplary solutions of the saddle point equations are plotted in Fig. 3. The interpretation of these plots is as follows: Each shown $\mu(x)$ is the most probable profile of the chemical potential inside the wire under the condition

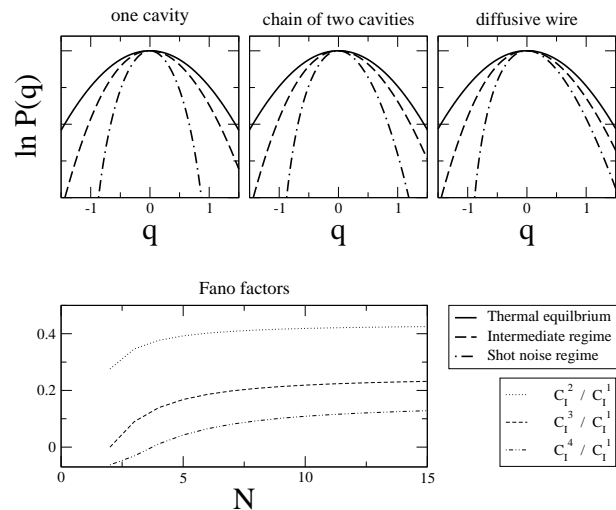


FIG. 4: *Upper panel:* Comparison of counting statistics of chaotic cavity, two cavities in series, and diffusive wire in the hot electron regime. We use the dimensionless variable $q = Q/(G \max\{\mu, \sqrt{3}T/\pi\}\tau)$ to parametrize the charge. For the intermediate case, we use the ratio $\mu/T = 2\pi/\sqrt{3}$. The distribution of charge in the shot noise regime is symmetric for a cavity, but asymmetric for a wire. *Lower panel:* Fano factors of second, third and fourth cumulant in the shot noise regime as a function of N , the number of point contacts in series.

that the charge $q = Q/(G\mu\tau)$ is measured after time τ . If for instance $q = 0$, i.e. the mean charge is measured, $\mu(x)$ has a linear profile. If the transmitted charge after a measurement is very small ($q = -0.9$), the potential drop occurs mostly in the middle of the wire: charges entering from the left therefore most likely diffuse back to the reservoir they have come from, before they follow the gradient of the chemical potential. If the transmitted charge is large ($q = 2.0$), the drop occurs mostly close the reservoirs. This means that many charge carriers from the left side are attracted to the middle of the wire, and escape to the right.

The upper panel of Fig. 4 compares the FCS of a cavity, of a chain of two cavities, and of a diffusive wire in the hot electron regime. It shows the distributions of transmitted charge $P(q)$ in thermal equilibrium $\mu \ll T$, for high bias $\mu \gg T$ and for an intermediate case $\mu/T = 2\pi/\sqrt{3}$. For zero temperature, the distributions are bounded from below and except for the wire also from above. For finite temperatures, the distributions acquire exponential tails. The most striking difference between the zero-dimensional cavity and the one-dimensional wire appears in the shot noise limit in which the distribution for the cavity becomes symmetric whereas the distribution for the wire stays asymmetric.

The lower panel of Fig. 4 illustrates the behavior of the Fano factors at zero temperature $F_n = C_n^n / C_1^1$ of several cumulants as a function of N , the number of point contacts. The result for F_2 is taken from Ref. 13. The results

for F_3 and F_4 are new, in the diffusive limit $N \rightarrow \infty$, F_3 agrees with the literature¹⁸. The increase of F_3 towards the diffusive limit describes the growing asymmetry of the charge distribution, the sign change of F_4 indicates that tails become more important in the diffusive limit.

IV. CONCLUSIONS

In this article, we presented a method to calculate the full counting statistics of semiclassical mesoscopic conductors in which electron-electron scattering is important. This method is based on a separation of time scales: The correlation time of extraneous sources of noise - such as the point contacts leading into a chaotic cavity or impurity scatterers in diffusive wires - is short compared to the characteristic time scales for the evolution of the electron distribution function. This allowed us to employ a stochastic path integral for the generating function of counting statistics which can be solved in saddle point approximation²⁰.

We derived a variety of results: For a chaotic cavity in the hot electron regime, the generating function of full counting statistics is given analytically. For this system we find that the thermalization of the electron gas in the cavity tends to symmetrize the probability distribution of counted charge. Whereas even cumulants are proportional to the maximum of external temperature and applied bias, odd cumulants are proportional to the minimum and vanish therefore in the shot noise regime. To the contrary, for a diffusive wire in the hot electron regime our numerical calculations show that this symmetrization does not exist. Furthermore, we discussed the frequency dependence of the third order correlation function and explained its unexpected low-frequency dispersion by charge-neutral fluctuations of the local electron temperature.

We stress the experimental importance of our findings: Noise measurements in wires with strong electron-electron scattering have been carried out with great precision^{10,11}. The resistances of the samples used in these experiments range from 1 to 300 Ω . The first successful measurement of a third cumulant² was carried out within this range. The third moment of FCS for diffusive wires in the hot electron regime should therefore be measurable in a similar setup. The chaotic cavities used in the experiments^{12,13} had higher resistances and would require a different setup to measure the third moment. The low-frequency dispersion sets in at an inverse dwell time $(\tau_d)^{-1}$ which we estimate from Ref. 12 to be 1-10GHz. Dispersion might therefore be of importance, since the bandwidth used in experiment² is of the same order.

As a final remark we would like to note that heating effects due to electron-electron scattering may not only occur inside a cavity or a diffusive wire, but also inside reservoirs. Most calculations (including the one presented in this article) assume reservoirs to be at local thermal equilibrium. This is completely justified for the electrochemical potential, since the electromagnetic signal propagates quickly throughout the reservoir. However, fluctuations of the electron temperature can be important at high frequencies, because their relaxation is much slower. Such temperature fluctuations in the reservoirs may couple back into higher order correlation functions of the electrical signal and may cause a low-frequency dispersion similar to the dispersion that we described in this article. In such cases, the notion of an ideal reservoir at local thermal equilibrium has to be given up.

We would like to thank E. V. Sukhorukov, K. E. Nagaev, and M. Kindermann for inspiring discussions and acknowledge support from the Swiss National Science Foundation.

-
- ¹ Ya. M. Blanter and M. Büttiker, *Physics Reports* **336**, 1-166 (2000).
- ² B. Reulet, J. Senzier, and D. E. Prober, *cond-mat/0302084* (2003).
- ³ C. W. J. Beenakker, M. Kindermann, and Yu. V. Nazarov, *Phys. Rev. Lett.* **90**, 176802 (2003).
- ⁴ L. S. Levitov and G. B. Lesovik, *Pis'ma Zh. Eksp. Teor. Fiz.* **58** (3), 225 (1993) [*JETP Lett.* **58**, 230 (1993)].
- ⁵ A. V. Andreev and E. G. Mishchenko, *Phys. Rev. B* **64**, 233316 (2001).
- ⁶ D. A. Bagrets and Yu. V. Nazarov, *Phys. Rev. B* **67**, 085316 (2003).
- ⁷ D. A. Bagrets and Yu. V. Nazarov, *cond-mat/0304339* (2003).
- ⁸ M. Kindermann, Yu. V. Nazarov, and C. W. J. Beenakker, *Phys. Rev. Lett.* **90**, 246805 (2003).
- ⁹ M. Kindermann and Yu. V. Nazarov, *cond-mat/0304078* (2003).
- ¹⁰ A. H. Steinbach, J. M. Martinis, and M. H. Devoret, *Phys. Rev. Lett.* **76**, 3806 (1996).
- ¹¹ M. Henny, S. Oberholzer, C. Strunk, and C. Schönberger, *Phys. Rev. B* **59**, 2871 (1999).
- ¹² S. Oberholzer, E. V. Sukhorukov, C. Strunk, C. Schönberger, T. Heinzel, and M. Holland, *Phys. Rev. Lett.* **86**, 2114 (2001).
- ¹³ S. Oberholzer, E. V. Sukhorukov, C. Strunk, and C. Schönberger, *Phys. Rev. B* **66** (2002) 233304.
- ¹⁴ K. E. Nagaev, *Phys. Rev. B* **52**, 4740 (1995).
- ¹⁵ V. I. Kozub and A. M. Rudin, *Phys. Rev. B* **52**, 7853 (1995).
- ¹⁶ M. J. M. de Jong and C. W. J. Beenakker in *Mesoscopic Electron Transport*, L. P. Kouwenhoven, G. Schön, and L. L. Sohn eds., NATO ASI Series E, Vol. 345 (Kluwer Academic, Dordrecht 1996).
- ¹⁷ E. V. Sukhorukov and D. Loss, *Phys. Rev. B* **59**, 13054 (1999).
- ¹⁸ D. B. Gutman and Y. Gefen, *Phys. Rev. B* **68**, 035302 (2003).

- ¹⁹ K. E. Nagaev, Phys. Rev. B **66**, 075334 (2002).
- ²⁰ S. Pilgram, A. N. Jordan, E. V. Sukhorukov, and M. Büttiker, Phys. Rev. Lett. **90**, 206801 (2003).
- ²¹ K. E. Nagaev, S. Pilgram, and M. Büttiker, cond-mat/0306465 (2003).
- ²² I. L. Aleiner, P. W. Brouwer, and L. I. Glazman, Phys. Rep. **358**, 309 (2002); and references therein.
- ²³ see C. W. J. Beenakker, Rev. Mod. Phys. **69**, 731 (1997) for further reading.
- ²⁴ Here it is implicitly assumed that diffraction is strong, in other words that the Ehrenfest time is much shorter than the dwell time of electrons in the cavity.
- ²⁵ M. Büttiker, H. Thomas, and A. Prêtre, Phys. Lett. A **180**, 364 (1993).
- ²⁶ R. A. Jalabert, J.-L. Pichard, and C. W. J. Beenakker, Europhys. Lett. **27**, 255 (1994).
- ²⁷ V. A. Khlus, Zh. Eksp. Teor. Fiz. **93**, 2179 (1987) [Sov. Phys. JETP **66**, 1243 (1987)].
- ²⁸ G. B. Lesovik, Pis'ma Zh. Eksp. Teor. Fiz. **49**, 513 (1989) [JETP Lett. **49**, 592 (1989)].
- ²⁹ M. Büttiker, Phys. Rev. B **46**, 12485 (1992).
- ³⁰ S. A. van Langen and M. Büttiker, Phys. Rev. B **56**, R1680 (1997).
- ³¹ Ya. M. Blanter and E. V. Sukhorukov, Phys. Rev. Lett. **84**, 1280 (2000).
- ³² Ya. M. Blanter, H. Schomerus, and C. W. J. Beenakker, Physica (Amsterdam) **11E**, 1 (2001).
- ³³ K. E. Nagaev, P. Samuelsson, and S. Pilgram, Phys. Rev. B **66**, 195318 (2002).
- ³⁴ M. Kindermann and S. Pilgram, cond-mat/0312430.
- ³⁵ The stochastic path integral approach can be applied to the cold electron regime as well. In this case, the occupation function $f_C(\varepsilon - U_C)$ fluctuates independently in each energy interval $d\varepsilon$ because single particle energy is conserved. For more details see Ref. 20. The curves for Fig. 2 were obtained in this way. Alternatively, the cumulants may be obtained from a quantum mechanical calculation: The FCS for non-interacting electrons in terms of transmission probabilities⁴ may be averaged over the distribution of transmission eigenvalues for an open chaotic cavity (this distribution was determined in Refs. 26,39 and can be found in review 23).
- ³⁶ E. V. Sukhorukov and S. Pilgram, unpublished.
- ³⁷ The generalization to higher dimensions is straightforward. A similar non-linear field theory can also be derived to describe the FCS of a diffusive conductor in the cold electron regime.⁴⁰
- ³⁸ We use an iterative Newton scheme to solve the nonlinear field equations.
- ³⁹ H. U. Baranger and P. A. Mello, Phys. Rev. Lett. **73**, 142 (1994).
- ⁴⁰ A. N. Jordan, E. V. Sukhorukov, and S. Pilgram, unpublished.